

# Negative Stiffness Honeycombs for Recoverable Shock Isolation

D. M. Correa, T. D. Klatt, S. A. Cortes, M. R. Haberman, D. Kovar, and C. C. Seepersad  
The University of Texas at Austin

## Abstract

Negative stiffness honeycomb materials are comprised of unit cells that exhibit negative stiffness or snap-through-like behavior. Under an external load of small magnitude, a negative stiffness honeycomb exhibits large effective elastic modulus, equivalent to those of other standard honeycomb topologies. When the external load reaches a predetermined threshold, the negative stiffness cells begin to transition from one buckled shape to another, thereby absorbing mechanical energy and mechanically isolating the underlying structure. When the external load is released, the honeycomb returns to its original topology in a fully recoverable way. In this paper, theoretical and experimental behavior of negative stiffness honeycombs is explored, based on FEA modeling and experimental evaluation of laser sintered specimens. Additive manufacturing enables fabrication of these complex honeycombs in regular or conformal patterns. Example applications are also discussed.

## Introduction and Background

Conventional cellular materials, such as hexagonal honeycombs, absorb energy by plastic deformation, which renders the absorbed energy unrecoverable and prevents reuse of the honeycombs. When subjected to a compressive force, as shown in Figure 1 [1], conventional honeycombs initially exhibit elastic deformation, followed by plastic buckling of the cell walls, which creates a relatively flat plateau stress region as the cells collapse, row by row. After all of the cells collapse fully, densification occurs leading to a sudden increase in stress levels. The force threshold and inherent elastic/plastic behavior of the cells can be controlled by modifying the cell geometry. Cell geometries with very low relative densities can exhibit elastic buckling of the cells under compressive loading, whereas plastic buckling occurs at higher relative densities. However, manufacturing cells with extremely low relative densities using additive manufacturing techniques is difficult due to the inherent dimensional limitations of most commercially available machines. Low density materials also possess low stiffness and buckle under loads of lesser magnitude.

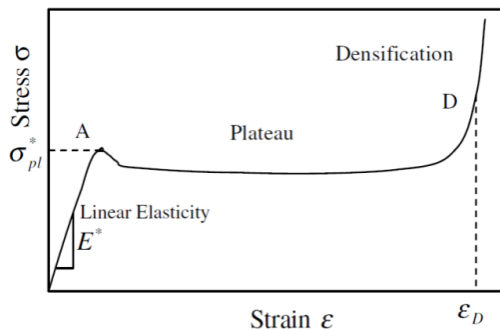


Figure 1: Mechanical behavior of honeycombs [1].

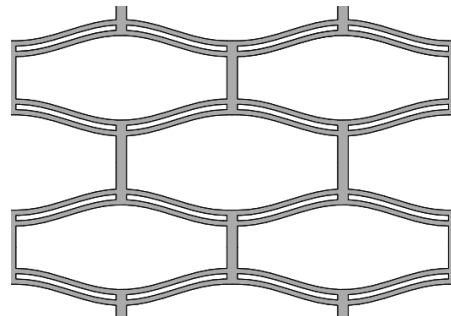


Figure 2: Negative stiffness honeycomb.

In contrast to conventional honeycombs, negative stiffness honeycombs exhibit a combination of high initial stiffness and recoverable energy absorption. The negative stiffness honeycombs are comprised of alternating negative stiffness beams, arranged in a repeating pattern, as shown in Figure 2. Negative stiffness beams allow for energy recovery as they deform from one first-mode-buckled shape to another, exhibiting negative stiffness properties along the way. They tend to exhibit high initial stiffness and also offer nearly ideal shock isolation at designed force thresholds. Evaluation of the performance of a single negative stiffness beam was performed by Klatt [2] based on the work of Qiu et al. [5] and former University of Texas students Fulcher [3] and Kashdan [4]. Klatt showed that prefabricated curved beams (Figure 3) can be used to achieve negative stiffness behavior, similar to the negative stiffness behavior typically exhibited by straight beams subject to buckling by axial loads. According to Qiu, the force-displacement relationship for a pre-curved beam is:

$$F = \frac{3\pi^4 Q^2}{2} \Delta \left( \Delta - \frac{3}{2} + \sqrt{\frac{1}{4} - \frac{4}{3Q^2}} \right) \left( \Delta - \frac{3}{2} - \sqrt{\frac{1}{4} - \frac{4}{3Q^2}} \right) \quad (1)$$

where  $\Delta$  represents normalized displacement and  $Q$  represents the ratio between  $h$ , the apex height of the beam, and  $t$ , the thickness of the beam. Using this equation, Qiu plotted various force-displacement diagrams (see Figure 4) by varying the geometry constant  $Q$ . It is obvious from the plots obtained that an increase in  $Q$  leads to pronounced negative stiffness behavior in the beam.

Klatt fabricated pre-curved beams using selective laser sintering and performed compression testing on them. Figure 5 shows the experimental results obtained by Klatt. It is clear that the beam exhibits negative stiffness near the end of its loading path. It is also clear that the unloading path differs from the loading path, which indicates that energy is being dissipated within the material as it deforms from one position to the other.

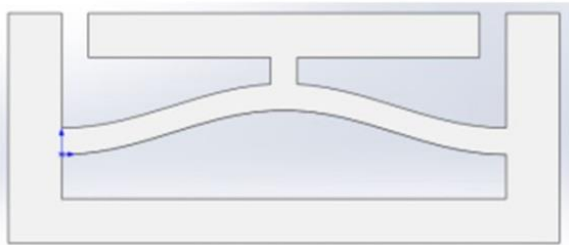


Figure 3: A precurved beam used as a negative stiffness beam in Klatt's study [2].

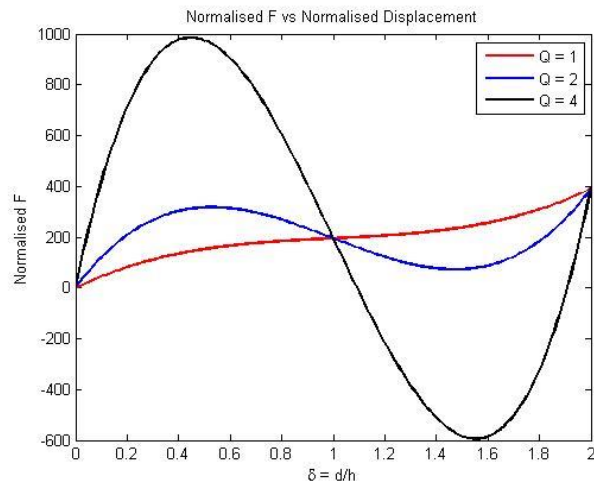


Figure 4: Various force-displacement curves obtained by varying  $Q$  in Eq. 1.

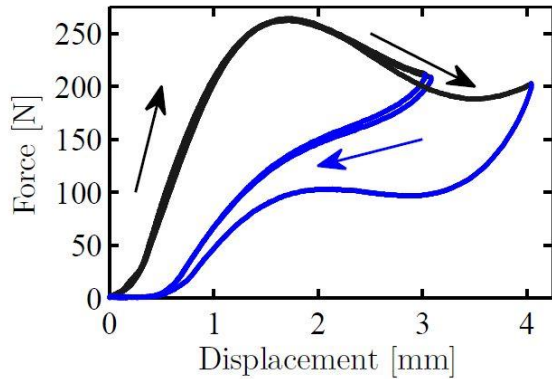


Figure 5: Experimental results obtained by Klatt for a single negative stiffness element (Figure 3) with fixed boundary conditions and vertically oriented compressive loading [2]. The loading path is in black while the unloading path is in blue.

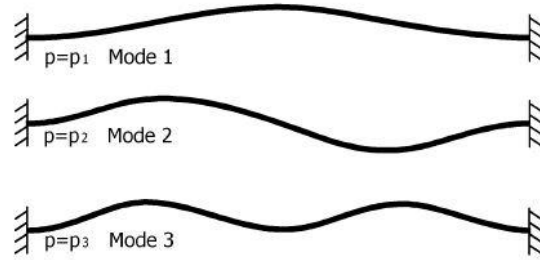


Figure 6: First three buckling modes of a curved beam [5].

When the curved beams shown in Figure 3 are placed in a repeating pattern, the beams tend to twist upon application of a compressive load and transition from one first-mode-buckled shape to another via the second mode shape illustrated in Figure 6. This twisting behavior prevents the honeycomb from exhibiting negative stiffness behavior. Restricting the curved beams to transition from one first-mode-buckled shape to another via the third-mode-buckled shape preserves each beam's negative stiffness behavior. Using two concentric curved beams clamped to one other is one way to force the beam to transition between first-mode-buckled shapes via third mode buckling. Therefore, the negative stiffness honeycombs presented in the next section consist of double beams arranged in an alternating pattern to create a honeycomb structure. The behavior of the honeycomb can be controlled by adjusting the beam geometry, particularly the ratio  $Q$  described earlier.

### 3D Modeling, Designing, and Prototyping

An initial prototype for the negative stiffness honeycomb is illustrated in Figure 7. The prototype was printed using a MakerBot Replicator 2 in PLA (polylactic acid) material. During compression testing, the prototypes were supported by a customized fixture, illustrated on the right side of Figure 7, which prevented horizontal expansion of the honeycomb upon application of a vertically oriented compressive load. Without this reinforcement, the honeycombs would expand horizontally, and negative stiffness behavior would be lost. However, the fixture supported only the cell walls along the boundary of the honeycomb, while the vertical cell walls in the interior of the part were free to translate and rotate. Furthermore, friction between the fixture and the honeycomb impacts the force-displacement behavior. These unintended phenomena made it difficult to observe negative stiffness behavior during physical testing, prompting revisions to the honeycomb design.

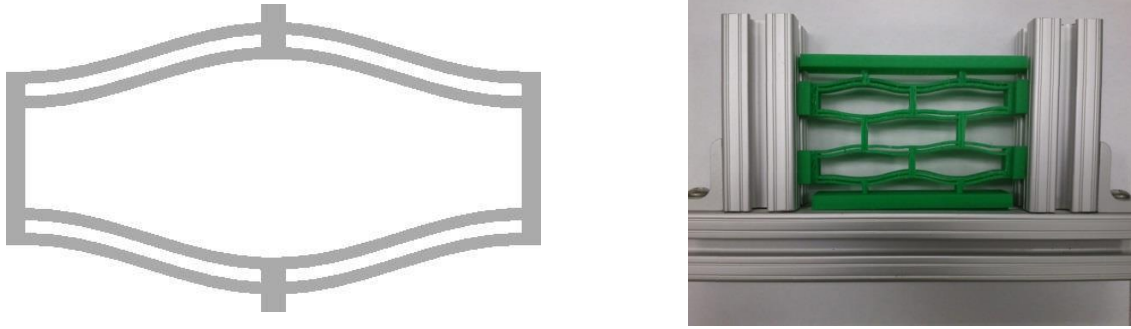


Figure 7: Primitive negative stiffness cell (left) and negative stiffness honeycomb in a supporting fixture (right).

The revised design is illustrated in Figures 8 and 9. The prototype was fabricated with a 3D Systems HiS-HiQ Vanguard selective laser sintering (SLS) machine and nylon 11 material. The dimensions of each individual cell are documented in Figure 8. The relative density of the design was calculated to be 0.1766.

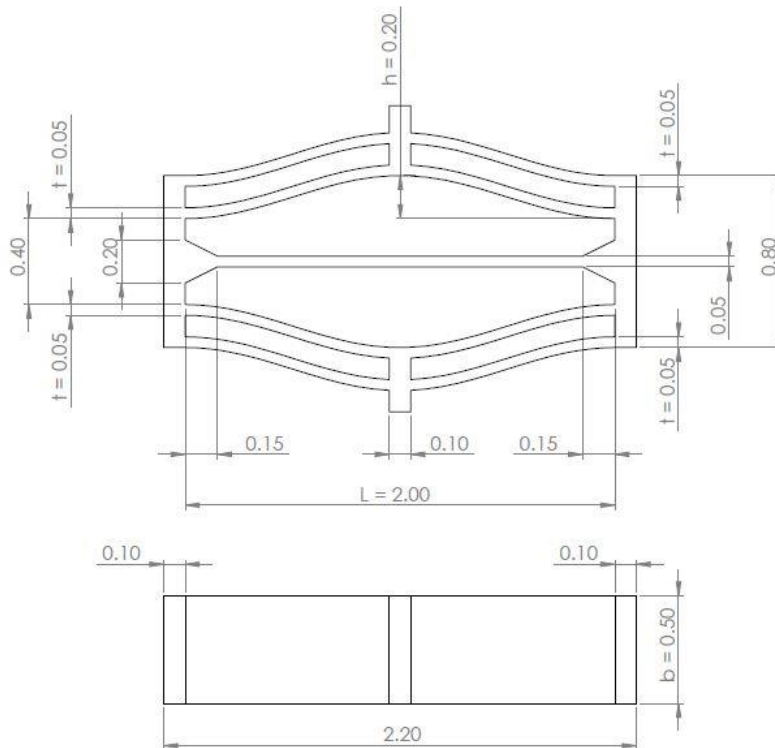


Figure 8: Geometry of a revised negative stiffness unit cell.

As shown in Figure 8, the cell has a rigid central beam that helps prevent rotation and lateral expansion of the vertical cell walls, which limit negative stiffness behavior. The rigid central beam also eliminates the need for a supporting fixture, rendering the honeycomb fixtureless. A series of identical cells of this type are stacked together to create a negative stiffness honeycomb as shown in Figure 9. The physical prototype built in SLS is illustrated in Figure 10. The fact that

the improved design does not need to be supported in a fixture means that it can be used in a variety of applications such as helmets and packaging where it may not always be possible to provide transverse support to the honeycomb.

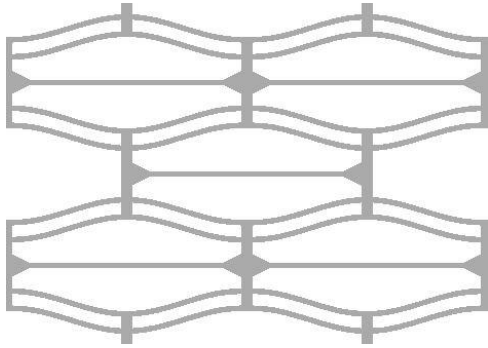


Figure 9: Revised negative stiffness honeycomb with central beams.

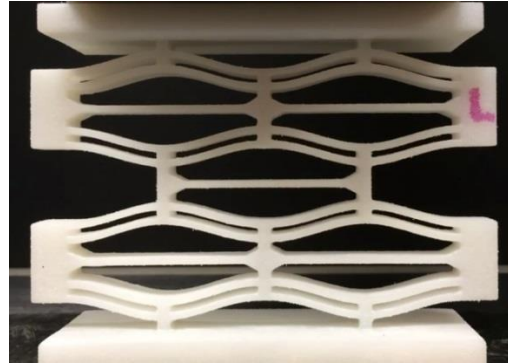
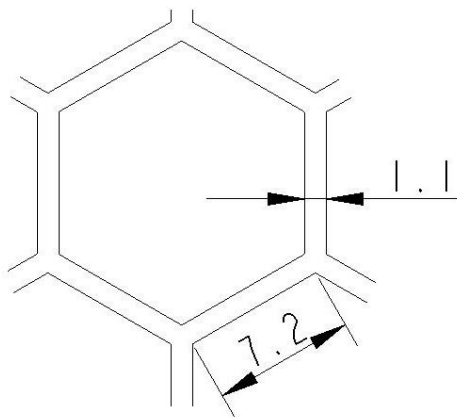


Figure 10: Revised negative stiffness honeycomb design embodied in SLS and nylon 11.

To compare the performance of the negative stiffness honeycomb to a regular hexagonal honeycomb, a prototype of the latter was built with the same relative density as the negative stiffness honeycomb. The prototype was fabricated with a 3D Systems HiS-HiQ Vanguard selective laser sintering (SLS) machine and nylon 11 material. The cell design parameters are documented in Figure 11. The honeycomb was designed to exhibit a plateau stress similar in magnitude to the force threshold of the NS honeycomb.



Parameter	Symbol	Value	Unit
Length	L	7.2	mm
Thickness	t	1.1	mm
Width	b	7.9	mm

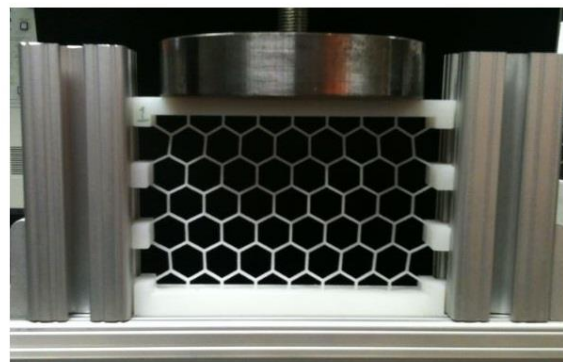


Figure 11: Hexagonal honeycomb with equivalent relative density: cell dimensions (left) and prototype (right).

## Finite Element Analysis

To predict the performance of the NS honeycomb under a vertically oriented compressive load, finite element analysis in COMSOL was performed. The analysis was idealized by supporting each of the vertical cell walls with roller supports (simulating the effect of a rigid central beam without actually having a beam in the model), as shown in Figure 12. Displacement-controlled loading was applied at the top surface and a fixed support provided to the bottom surface.

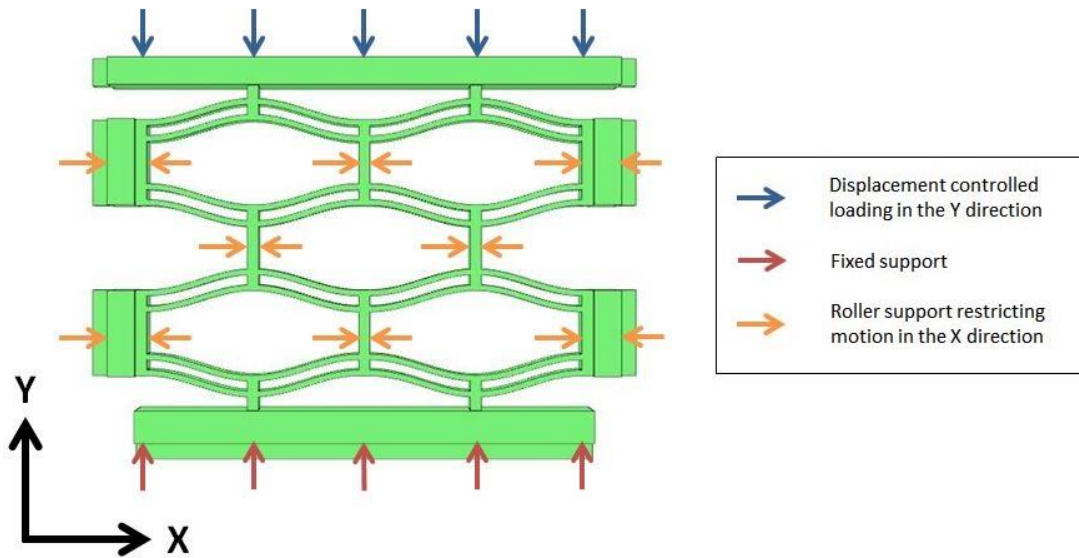


Figure 12: Idealized loading of negative stiffness honeycomb for COMSOL analysis.

The Young's modulus of laser sintered nylon 11 was determined by building tensile bars along with the honeycombs. The resulting properties are summarized in Table 1. These properties are determined by averaging the Young's moduli of multiple tensile bars built near the honeycomb in the build chamber.

Property	Value	Unit
Density	1040	kg/m <sup>3</sup>
Poisson's Ratio	0.33	-
Young's Modulus	1582	MPa

Table 1: Properties of laser sintered nylon 11 for COMSOL analysis

The predicted force-displacement relationship from FEA reveals repeating negative stiffness regions in Figure 13. Each negative stiffness region is caused by a single row of curved beams transitioning from one first-mode-buckled shape to another. The layers buckle sequentially. In practice, the order in which the layers buckle could be determined by relative imperfections or weaknesses in one or more beams, causing them to buckle under slightly less

compressive load than other layers. We can observe from the plot in Figure 13 that the force threshold reached before buckling begins to occur is approximately 275 N.

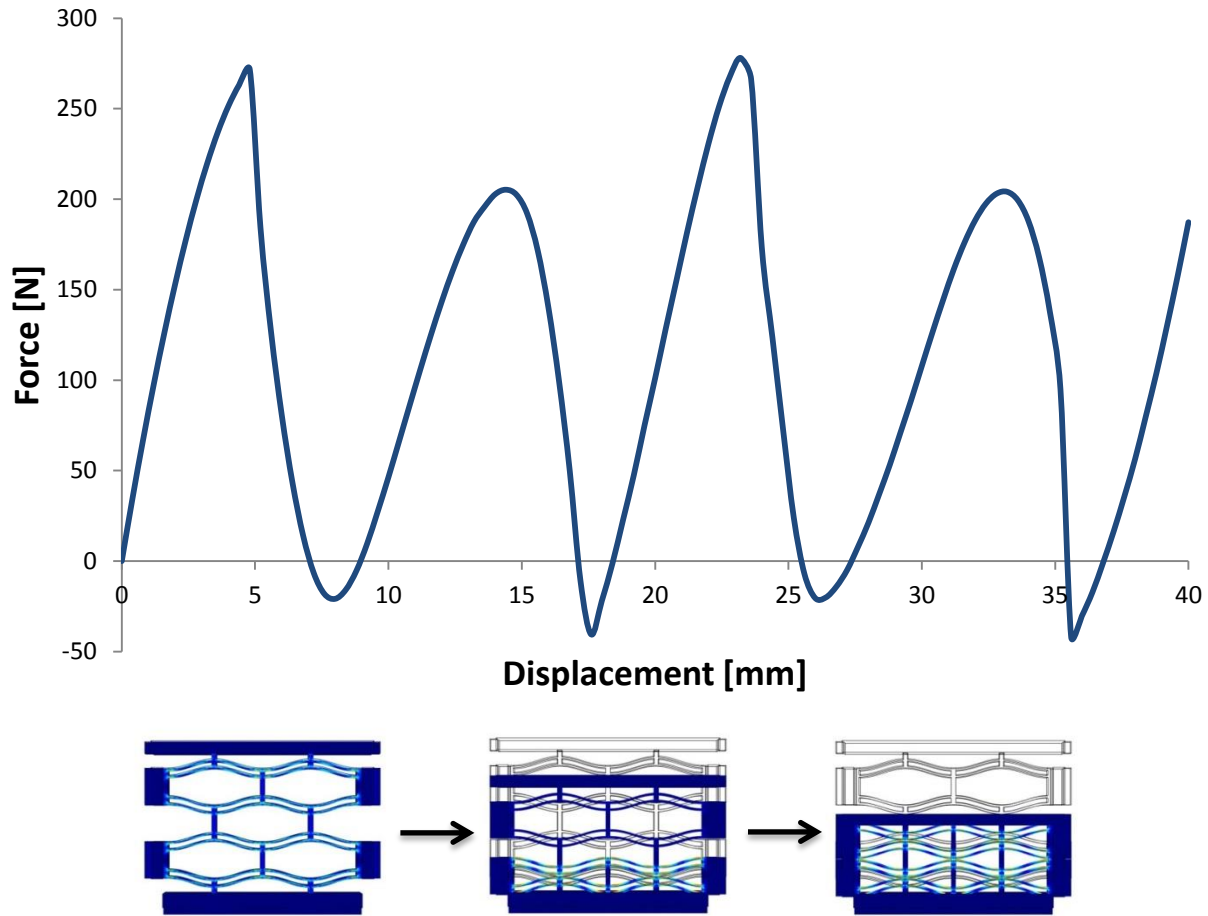


Figure 13: Force-displacement relationship of the revised design (seen in Figures 5 and 6) as simulated in COMSOL (top) and a sequence of schematics showing evolution of the structure during compressive loading (bottom).

## Experimental Results

The revised honeycomb prototypes were compression tested on a universal testing frame (MTS Sintech 2G). A total of two prototypes were tested, and each prototype was tested twice. The prototype was supported between the crosshead of the machine and its base without the use of a supporting fixture as explained previously. A compressive displacement of 35 mm was applied to each prototype at a constant crosshead velocity of 5 mm/min. Displacements greater than 35 mm resulted in densification of the prototype with a corresponding sharp increase in force; therefore, displacements beyond 35 mm were avoided in the experiments. The force-displacement data was recorded for one complete cycle of loading and unloading for each test.

A prototype in various stages of compression is shown in Figure 14, and experimental force-displacement data is plotted in Figure 15. As shown in Figure 14, the layers buckle sequentially but in no particular order. Inherent inconsistencies in the material may cause different layers to exhibit different force thresholds and buckle before others. Figure 15 shows successive regions of negative stiffness behavior as each layer of the honeycomb buckles from

its first mode position to its diametrically opposite first mode position via third mode buckling. This trend corresponds to the FEA predictions.

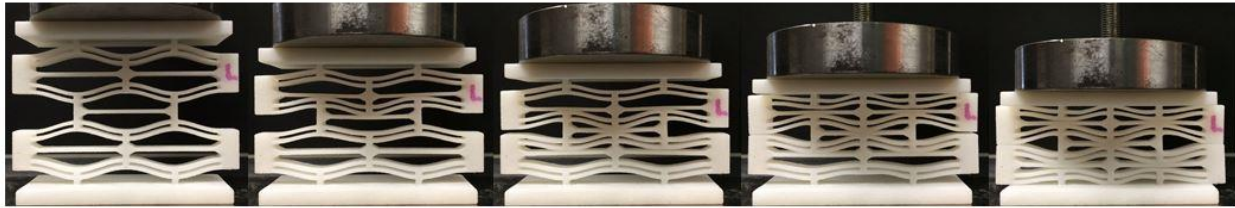


Figure 14: An SLS prototype of the revised negative stiffness honeycomb in various stages of compression.

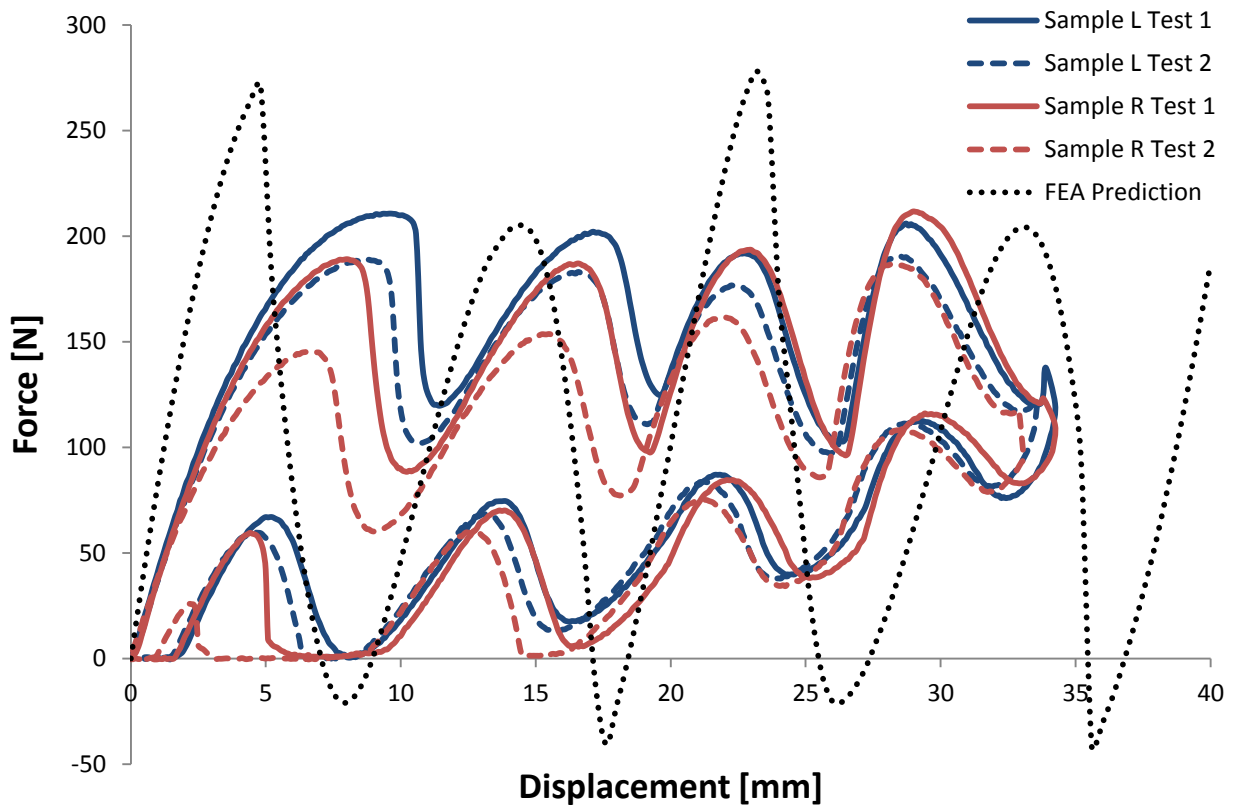


Figure 15: Force-displacement relationships for the SLS prototypes of the revised negative stiffness honeycomb.

The FEA predictions and experimental data differ with respect to the magnitudes of the reaction forces exhibited by the honeycombs. The experimental force threshold is approximately 200 N, compared to the FEA prediction of approximately 275 N. Also, the physical specimens exhibit negative stiffness over a much smaller range of forces and displacements. These differences may be explained by several factors. First, the visco-elastic behavior of the nylon 11 material is not captured in the FEA models. Second, there could be some plastic deformation occurring in regions of the part with high stress concentrations (e.g., joints). Finally, the

horizontal beams are assumed to be rigid in the FEA, but they undergo non-negligible deformation in the physical specimens.

It is apparent in Figure 15 that the loading and unloading paths of the prototype are not equivalent. The difference between the areas under the loading and unloading curves is the energy absorbed by the honeycomb over the complete cycle of loading and unloading. The amount of energy absorbed can be calculated by numerically integrating the force with respect to displacement using the data generated from the physical tests. The integration was carried out in MATLAB using trapezoidal integration and the results are presented in Table 2.

The degree of permanent deformation in the tested samples is tabulated in Figure 16. As further evidence that the negative stiffness honeycombs provide recoverable energy absorption, the dimensional changes in the heights of the prototypes after two cycles of complete loading and unloading were negligible (0.2 - 0.5%).

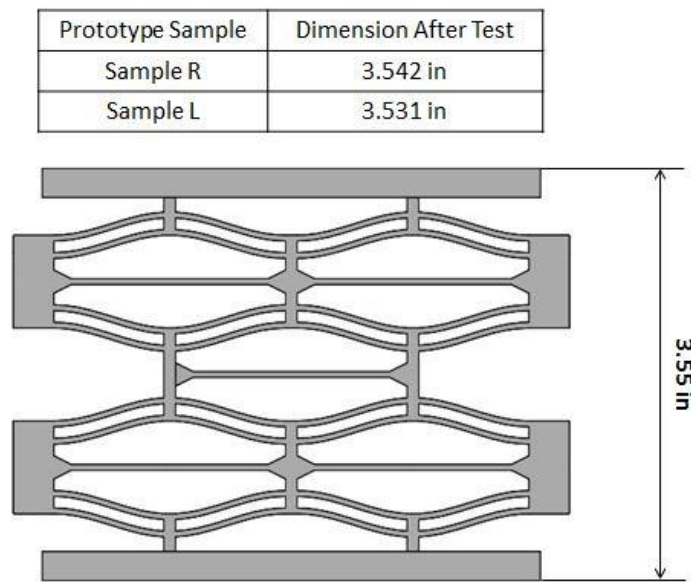


Figure 16: Measure of permanent deformation in the negative stiffness prototypes.

As a comparison, a hexagonal honeycomb prototype of equivalent relative density was tested. The honeycomb was configured to absorb energy at a force threshold very similar to that of the negative stiffness honeycomb. The stage-wise compression of the hexagonal honeycomb can be seen in Figure 17. A plot of vertical displacement versus compressive force is shown in Figure 18. The results reveal a force threshold of approximately 400 N and a plateau region in the range of 200 to 250 N, which is similar to that obtained with the negative stiffness honeycomb. As shown in Table 2, the hexagonal honeycomb recovers very little from its collapse, returning approximately 10% of the energy absorbed and remaining in a plastically deformed, collapsed configuration.

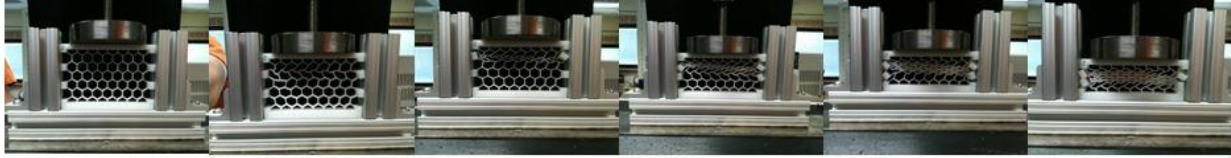


Figure 17: An SLS hexagonal honeycomb prototype in various stages of compression.

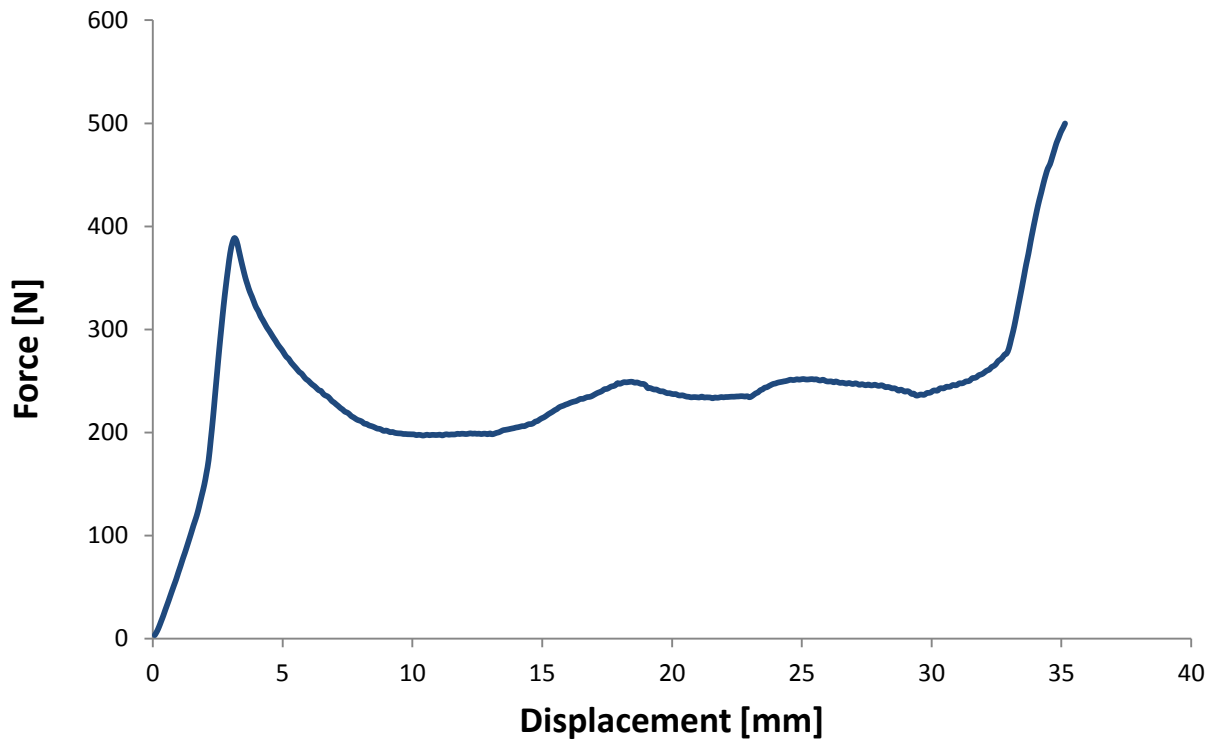


Figure 18: Force-displacement relationship of the SLS hexagonal honeycomb.

Prototype Sample	Test	Energy Absorbed During Loading [J]	Energy Recovered During Unloading [J]	Net Energy Absorbed [J]	Percent Energy Absorbed [%]	Mass [g]	Energy Absorbed Per Unit Mass [mJ/g]
Sample R	Test 1	4.88	1.62	3.26	66.8	24.74	131.8
	Test 2	3.91	1.33	2.58	66.0	24.74	104.3
Sample L	Test 1	5.31	1.79	3.52	66.3	24.74	142.3
	Test 2	4.73	1.67	3.06	64.7	24.74	123.7
Hexagonal Honeycomb	Test 1	11.33	1.59	9.74	85.9	9.78	995.9

Table 2: Energy absorption results from numerical integration in MATLAB.

Table 2 also includes data on the mass of each specimen and the energy absorbed per unit mass. The mass represents the mass of the honeycomb cells alone, minus the additional material added to the top and bottom surfaces of the honeycombs for fixturing and uniform compression. As shown, the hexagonal honeycomb absorbs more energy per unit mass than the negative stiffness honeycomb specimens. The higher levels of energy absorption are explained partly by the permanent deformation and lack of energy recovery exhibited by the hexagonal honeycomb. Another important point is that the negative stiffness honeycombs have not yet been optimized to maximize energy absorption per unit mass.

## **Conclusions**

The negative stiffness honeycombs behave very similarly to regular honeycombs under compressive loading, with a linear initial stiffness followed by a region of nearly-constant-force energy absorption prior to densification. The advantage of the negative stiffness honeycombs is recovery; they recover their original shape and dimensions despite undergoing compression to the point of densification. Furthermore, this energy absorption can be designed to occur at a predetermined force threshold by altering the beam geometry. Layers can also be built with varying stiffness. The energy absorbed by the present design of the negative stiffness honeycombs is in the range of 64 to 67% of the energy input to them, with net energy absorbed in the range of 2.5 to 3.5 J. For a similar force threshold, a regular honeycomb with similar relative density absorbed approximately 9.7 J of energy but was permanently deformed in the process.

The negative stiffness honeycombs can find suitable applications in impact protection devices, such as helmets, bumpers, and blast mitigation devices. The energy absorbing capabilities coupled with the complete recoverability of the honeycombs can be leveraged to create longer lasting impact protection devices. The recoverability of the honeycombs can be exploited to develop reusable packaging that is capable of withstanding repeated impacts while protecting the contents of the package. The devices can also be made to isolate shocks at a designed force threshold. This property could be very useful for protecting occupants from impacts exceeding an injury limit, as in suspension systems or protective gear.

## **Acknowledgements**

We are grateful to Summer Gunnels, Mike Orr, Ellyn Ranz, and Mark Phillips for their assistance in this work.

## **References**

1. Hayes, A. M., Wang, A., Dempsey B. M., McDowell, D. L., 2004. Mechanics of Linear Cellular Alloys. *Mechanics of Materials* 36, pp. 691-713.
2. Klatt, T. D., 2013. Extreme Energy Absorption: The Design, Modeling, and Testing of Negative Stiffness Metamaterial Inclusions. Master's Thesis, The University of Texas at Austin.

3. Fulcher, B.A., 2012. Evaluation of Systems Containing Negative Stiffness Elements for Vibration and Shock Isolation. Master's Thesis, The University of Texas at Austin.
4. Kashdan, L. B., 2010. Evaluation of Negative Stiffness Elements for Enhanced Material Damping Capacity. Master's Thesis, The University of Texas at Austin.
5. Qiu, J., Lang, J. H., Slocum, A. H., 2004. A Curved-Beam Bistable Mechanism. *Journal of Microelectromechanical Systems* Vol. 13, No. 2, pp. 137-146.